



# Changes of vegetation carbon sequestration in the tableland of Loess Plateau and its influencing factors

Jie Zhang<sup>1</sup> · Mengyun Liu<sup>1</sup> · Mengmeng Zhang<sup>1</sup> · Jinghan Yang<sup>1</sup> · Runshan Cao<sup>1</sup> · Sukhdev S. Malhi<sup>2</sup>

Received: 28 August 2018 / Accepted: 23 May 2019 / Published online: 30 May 2019  
© Springer-Verlag GmbH Germany, part of Springer Nature 2019

## Abstract

The variations of vegetation carbon sequestration have become a gauge for evaluating the ecological effect of vegetation restoration. In this study, the spatiotemporal patterns of the net ecosystem production (NEP) were simulated using an improved CASA model and GSMSR model. It showed that the NEP markedly increased in the tableland of Loess Plateau during 2003–2012, with an annual average growth of  $3.65 \text{ g C} \cdot \text{m}^{-2} \text{ a}^{-1}$ . The mixed broadleaf-conifer forest ranked first ( $127.23 \text{ g C} \cdot \text{m}^{-2} \text{ a}^{-1}$ ) while the bare land and sparse vegetation presented the lowest carbon sequestration ( $14.64 \text{ g C} \cdot \text{m}^{-2} \text{ a}^{-1}$ ). The NEP manifested a significantly uneven overall spatial distribution: high in the southwest and low in the northeast. The spatial variations of NEP resulted from the combined effects of geographic position, terrain, meteorology, and soil and vegetation, respectively. Quantitative isolation revealed that the most dominant factor of vegetation carbon sequestration was soil and vegetation, while terrain exerted insignificant impacts on the NEP.

**Keywords** NEP · CASA · GSMSR · Influencing factors · Tableland of Loess Plateau

## Introduction

The net carbon absorption or net carbon emission of a terrestrial ecosystem is called the net ecosystem productivity (NEP) (Woodwell et al. 1978). NEP reflects the difference between the net primary productivity (NPP) of vegetation in the ecosystem and the heterotrophic respiration (HR) of the soil (Zhao et al. 2009). Given that the NEP denotes the equilibrium between the photosynthesis and respiration of an ecosystem, it can reflect the  $\text{CO}_2$  amount absorbed from or released into the atmosphere by the ecosystem in unit time (Mu et al. 2014). Generally speaking, when the carbon sequestration of an ecosystem is greater than its carbon emission, this ecosystem is

considered a sink of atmosphere  $\text{CO}_2$  (carbon sink), otherwise, a carbon source (Fang et al. 2007). It was an important characteristic parameter in both ecosystem and a physical quantity in carbon exchange between terrestrial ecosystem and atmosphere.

Previous researchers in China (Liu et al. 2014; Piao et al. 2004) have evaluated the biomass carbon sink of forest and grassland, and they found that different vegetation types play different roles in the carbon cycle of an ecosystem. That is, grassland degeneration is typically a carbon source process (Chuluun and Ojima 2002), whereas afforestation increases the carbon storage of an ecosystem (Fang et al. 2001; Tian et al. 2011; Zhang et al. 2005). Studies have demonstrated that afforestation is the most promising strategy for mitigating global warming. The tableland of Loess Plateau is located in the area of northwest China, and the ecological environment is extremely fragile. Large-scaled afforestation activities have been conducted since the Three-North Shelter Forest Program (TNSFP) and Grain to Green Program (GTGP) were implemented in 1975 and 1999, respectively. The designation of agricultural protected forests significantly improved the local microclimate, crop yield, soil conditions, and air purification. Nevertheless, agricultural protected forests incurred severe losses and damages because few forest resources were scattered in local areas. The tableland of Loess Plateau is a

Responsible editor: Philippe Garrigues

✉ Mengyun Liu  
lmy471993@163.com

Jie Zhang  
zhangjie6076@163.com

<sup>1</sup> College of Natural Resources and Environment, Northwest A&F University, Yangling 712100, Shaanxi Province, China

<sup>2</sup> Department of Renewable Resources, University of Alberta, Edmonton, Alberta, Canada

major crop planting region in Shaanxi Province that must meet the basic grain supply and maintain a sustainable development of the local ecological environment. Various ecological reconstruction activities have been established to address this problem. In view of the local fragile ecological environment and the impact of human activities, by exploring the carbon cycle process of the ecosystem in the study area, we can effectively evaluate the benefits of ecological restoration projects such as TNSFP and GTGP. Carbon fluxes in previous estimates usually depend on approaches that are based on varied types and numbers of parameters because of the difficulty in directly obtaining NEP measured data (Mekonnen et al. 2016; Ma et al. 2017). Carnegie-Ames-Stanford Approach (CASA) model which combined with satellite remote sensing in time series prediction of NPP was introduced by Potter et al. (1993). However, uncertainties in the CASA model raised from parameters or datasets used to drive the model made it limited at the regional or global scale (PAN et al. 2015; Field et al. 1995; Russell et al. 1989). Later, scholars constantly revised the CASA model (Carvalho et al. 2010; Zhu et al. 2006, 2007). Approaches in evaluating  $R_s$  (soil respiration) were constructed based on the correlations between environmental variables and measured soil carbon flux at the regional scale were introduced in some papers (Raich and Potter 1995; Raich et al. 2002). Based on the  $R_s$  data measured in China from 1995 to 2004, Yu (Yu et al. 2010) developed a new region-scale geostatistical model of soil respiration (GSMSR) by parameterizing and modifying the structure of the TPS model (Zheng et al. 2010). In this paper, the spatial-temporal distribution characteristics of the NEP in the tableland of Loess Plateau during 2003–2012 were simulated by using the improved CASA model and the GSMSR model. In conclusion, the findings of this study are beneficial for the accurate evaluation of the vegetation restoration in the tableland of Loess Plateau and to the quantitative analysis of the effects of the relative factors on the vegetation carbon sink.

## Materials and methods

### Study area

The tableland is in the hinterland of the Guanzhong plain of Northwest China. This region is characterized mainly by valley terraces covered with loess and loess platforms in a strip distribution along the river valley. The area is located at 34° 02′–35° 52′ N 107° 1′–110° 36′ E, encompassing Baoji, Xianyan, Tongchuan, Weinan, and Xi'an (Fig. 1). The region has an east-to-west length of approximately 320 km and south-to-north width of approximately 210 km, covering an area of around 12,000 km<sup>2</sup>. The local terrain is high in the west and low in the east, showing a ladder slope. The region is characterized by a continental monsoon climate with seasonal

changes. The annual average temperature over the years is 12.2–13.4 °C, the average temperature in July was above 26 °C, and in January it was 0.5–1.5 °C, and the average precipitation is 560–760 mm. The good hydrothermal conditions in this region have resulted in diversified vegetation types, which include evergreen broad-leaf forest, deciduous broad-leaf forest, mixed broadleaf-conifer forest, shrub forest land, cultivated land, grassland, bare land, and sparse vegetation. The study area is a part of Guanzhong Plain (also known as Weihe Plain) in Shaanxi province. Since ancient times, irrigation has been developed and wheat and cotton have been produced. It is an important commodity grain-producing area in China. However, the study area has a fragile ecology because of the high population and industrial density.

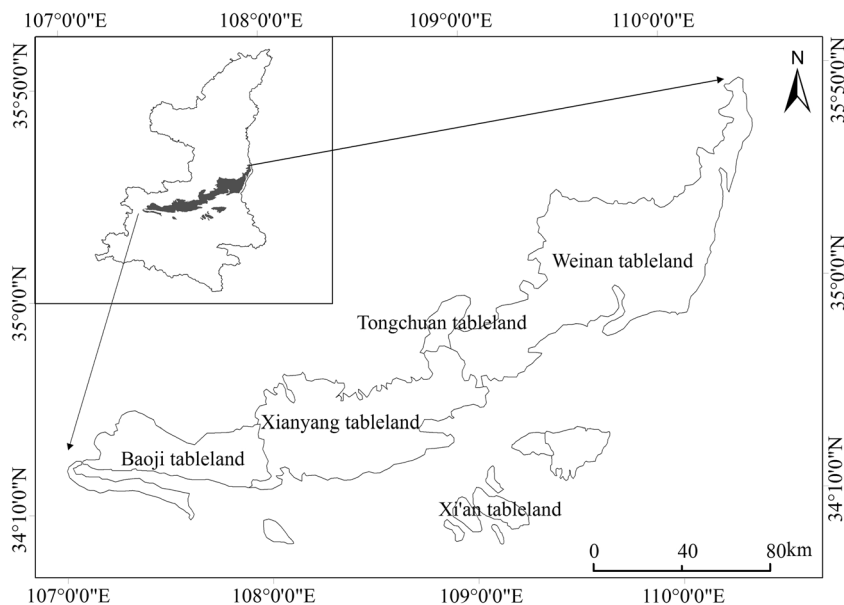
### Data sources and preprocessing

The meteorological data and coordinates of different stations were collected from China Meteorological Data Sharing Service System (<http://data.cma.cn>). The monthly data in the period of 2003–2012 were used. To obtain the spatial raster data of air temperature, precipitation, and solar radiation, the temperature data were interpolated by IDW (inverse distance weighted) method, and the precipitation and monthly total solar radiation data were assessed by OK (Kriging) method. The DEM data were acquired from the Geospatial Data Cloud website of the Computer Network Information Center, Chinese Academy of Science (<http://www.gscloud.cn>).

The normalized difference vegetation index (NDVI) utilized the SPOT VGT dataset issued by the Flemish Institute for Technological Research (<http://www.vgt.vito.be/>), and the spatial resolution was 1072.01946341615 m. The data were processed by geometric correction, radiation correction, and atmosphere correction. The 10-day maximum data were generated by the maximum value composite (Pan et al. 2003). The Band Math tools of ENVI were used again after the data were acquired to synthesize the maximum data and consequently weaken the influences of the atmosphere.

The used vegetation classification map was the China 1-km Land Coverage Map based on Multi-source Data Integration provided by the Cold and Arid Regions Science Data Center at Lanzhou (<http://westdc.westgis.ac.cn>) (Ran et al. 2009). The data applied the IGBP classification system, and the total accuracy of the region was 71%, which was higher than other data classification products, indicating that the data were suitable as the input data of a terrestrial model (Ran et al. 2012).

All data were resampled at a 1 km × 1 km resolution and repeatedly projected for WGS\_1984\_Albers. The north offset and east offset were 0 m. The central meridian was 105° E. The standard parallels were 25° N and 47° N. The initial latitude was 0°.

**Fig. 1** Location of the study area

## Methods

### Model description of NPP estimation

This study used the CASA model to estimate the monthly NPP of the vegetation in the tableland of the Loess Plateau in the period of 2003–2012. The NPP evaluated by the model was expressed as the product of the absorbed photosynthetically active radiation (APAR) and the actual radiation conversion efficiency ( $\epsilon$ ). The estimation formula is represented as follows:

$$\text{NPP}(x, t) = \text{APAR}(x, t) \times \epsilon(x, t) \quad (1)$$

where  $\text{APAR}(x, t)$  is the absorbed photosynthetically active radiation at  $t$  months for  $x$  grids ( $\text{MJ m}^{-2} \text{ month}^{-1}$ ) and  $\epsilon(x, t)$  is the actual radiation conversion efficiency at  $t$  months for  $x$  grids ( $\text{g C} \cdot \text{MJ}^{-1}$ ).

$$\text{APAR}(x, t) = \text{SOL}(x, t) \times \text{FPAR}(x, t) \times \alpha \quad (2)$$

where SOL is the global solar radiation at  $t$  months for  $x$  grids ( $\text{MJ m}^{-2} \text{ month}^{-1}$ ), FPAR is the absorption ratio of the vegetation layer to the incident photosynthetically active radiation, and the constant  $\alpha$  is the ratio of the effective solar radiation in the vegetation to the total global solar radiation.

$$\epsilon(x, t) = T_{\epsilon 1}(x, t) \times T_{\epsilon 2}(x, t) \times W_{\epsilon}(x, t) \times \epsilon_{\max} \quad (3)$$

where  $T_{\epsilon 1}(x, t)$  and  $T_{\epsilon 2}(x, t)$  are the temperature stress coefficients,  $W$  is the water stress coefficient, and  $\epsilon_{\max}$  is the maximum radiation conversion efficiency ( $\text{g C} \cdot \text{MJ}^{-1}$ ). Their computation functions can be found in the references (Zhu Zhu et al. 2007).

### Model description of Rh estimation

The GSMSR (Yu et al. 2010; Zhan et al. 2012;) is driven by monthly air temperature, monthly precipitation, and 0–20 cm soil organic carbon (SOC) density. This model can capture 64% of the spatiotemporal variability of soil  $R_s$  in China. The formula can be obtained after ascending dimension as follows:

$$\begin{aligned} R_{s, \text{month}} &= (0.588 + 0.118 \times \text{SOCD}) \\ &\times e^{\ln(1.83 \times e^{-0.006 \times T}) \times T \div 10} \times (P_1 \div 10 + 2.972) \\ &\div (P_1 \div 10 + 5.657) \times 30 \end{aligned} \quad (4)$$

where  $R_{s, \text{month}}$  is the monthly total soil respiration and  $P_1$  is the monthly total precipitation.

$$R_s = -0.0009R_h^2 + 0.6011R_h + 4.8874 \quad (5)$$

where  $R_h$  is the monthly soil heterotrophic respiration (HR).

Shi (2015) obtained the polynomial relationship model (formula 5) ( $R^2 = 0.6668$ ,  $P < 0.01$ ) by performing regression analysis based on the measured  $R_s$  and  $R_h$  data in China, which highly fitted to the original data. We used this model to calculate HR.

### Trend analysis of the NEP model

A unary linear regression analysis model based on generalized least squares was used to simulate the linear trend between the NEP and time. The overall variation trend of the time-series data was reflected by the slope of model, which can be expressed by the following equation (Ma et al. 2006):

$$\text{Slope} = \frac{n \times \sum_{i=1}^n (\text{NEP}_i \times i) - \sum_{i=1}^n \text{NEP}_i \sum_{i=1}^n i}{n \times \sum_{i=1}^n n^2 - (\sum_{i=1}^n i)^2} \quad (6)$$

where Slope is the trend of the slope of the NEP in the study area, n is the year span ( $n = 10$  in this study), and  $\text{NEP}_i$  is the annual NEP for year  $i$ . A slope value exceeding 0 indicated that the NEP increased over time, whereas a value lower than 0 denoted a decreasing trend. The significance level of the variation trend was estimated by Pearson coefficients based on the correlation analysis between the NEP and the years (Luo et al. 2012).

### NPP and HR validation

Accuracy test for the estimated NPP and HR was made by two methods in this paper: one is to compare with the measured data (Table 1). The other one is to compare with the value that simulated by other model (Fig. 2). A total of 234 data points in 2005 were selected to compare with the NPP value provided by Resource and Environment Data Cloud Platform (<http://www.resdc.cn/>) which simulated by the GLO-PEM model, as the picture shows, NPP simulated by two models had a good consistency ( $R^2 = 0.69$ ,  $P < 0.01$ ). We also estimated the  $R_s$  (soil respiration) of study area from April 2012 based on the TP model (Raich et al. 2002), and then simulated HR by using the model presented by Bong-Lamberty et al. (2010). A total of 263 HR data points were selected for comparison between two models ( $R^2 = 0.4$ ,  $P < 0.01$ ), which shows GSMSR model underestimated HR than TP model. As a result, an overestimation of NEP arose primarily from the lower HR estimates.

*DBF* deciduous broad-leaved forest, *GRA* grassland, *CUL* cultivated land, *EBF* evergreen broad-leaved forest, *BS* bare land and sparse vegetation, *SF* shrub forest, *MBF* mixed broadleaf-conifer forest

**Table 1** Comparison of simulated NPP/HR/NEP with previous studies

	References	EBF	DBF	GRA	CUL	MBF	SF	BS
NPP	Zhu et al. 2007	407–1913	114–1669	231	239–760	257–717	364	
	Yuan et al. 2014	600–3500	250–2500	100–727	–	250–2500	4–1200	0–250
	Sun and Zhu 2001	910–1340	250–700	150–240	–	250–1000	–	–
	Potter,1993	1027	315	180	288	316	469	115
	This paper	425.13	427.42	336.16	391.57	429.76	359.79	123
HR	Zhang et al. 2013	464.00	491.00	412.00	659.00	591.00	310.00	359.00
	This paper	298.83	315.02	295.55	298.26	302.53	298.46	108.36
NEP	Pang et al. 2012	41.60	57.50	17.50	31.80	24.20	41.70	0–20
	Ren et al. 2017	–	–	41.80	–	–	45.40	–
	Ma et al. 2017	79.00	62.00	–	–	30.00	–	–
	This paper	126.29	112.40	40.61	93.31	127.23	61.33	14.64

### RDA variance decomposition

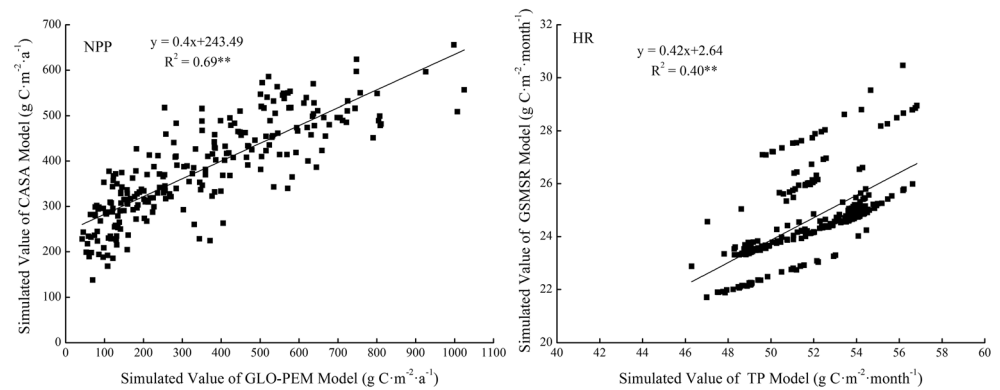
Redundancy analysis (RDA), an ordination analysis of ecological data using Vegan (vegetation analysis) Package in R (Oksanen et al. 2010), was performed to generate an intuitive quantitative description of the impacts of different factors (geographic position, terrain, meteorology, and soil and vegetation) on the NEP changes, which made up for the deficiency of only exploring the response of NEP to environmental factors in previous studies. Variance decomposition refers to the correlation and multi-element regression analyses between the NEP and the influencing factors. The influential gradient force reflects the importance of influencing factors to the NEP. For the quantitative analysis of the impacts of the different-dimensional environmental variables on the vegetation carbon sequestration efficiency in entire region, the average NEP in 10 years was used as the explained variable; longitude (LON), latitude (LAT), elevation (DEM), slope (SLO), aspect (ASP), temperature (TEM), rainfall (RF), solar radiation (RAD), vegetation index (NDVI), and soil organic carbon (SOC) were used as the explanatory variables. Variance decomposition and single-factor sequencing were performed to clarify the extent of influence of the different environmental variable groups on the vegetation carbon sequestration efficiency, as well as the extent of influence of each single factor.

### Results and analysis

#### Characteristics of inter-annual variation of vegetation carbon sequestration

As shown in Table 2, NPP value in the tableland of the Loess Plateau in the past 10 years was calculated by using the CASA model. The total NPP ranged from 4.75 Tg C to 5.40 Tg C during 2003–2012, with an average of 5.02 Tg C. The variation curve of the annual average NEP from 2003 to 2012 in the

**Fig. 2** Comparison of simulated NPP/HR with the value simulated by other model



study area (Fig. 3) showed that over the entire period, the variation of the NEP was consistent with that of the NPP. Whether it is NPP or NEP, they all show a fluctuating growth trend. The average NEP in the past 10 years was  $88.86 \text{ g C} \cdot \text{m}^{-2} \cdot \text{a}^{-1}$ . The minimum ( $64.00 \text{ g C} \cdot \text{m}^{-2} \cdot \text{a}^{-1}$ ) and maximum ( $118.87 \text{ g C} \cdot \text{m}^{-2} \cdot \text{a}^{-1}$ ) values were achieved in 2003 and 2010, respectively, with a range of  $54.87 \text{ g C} \cdot \text{m}^{-2} \cdot \text{a}^{-1}$ . The total annual NEP increased by 71% from 0.83 Tg C in 2003 to 1.42 Tg C in 2012.

### Characteristics of the seasonal variations of vegetation carbon sequestration

The monthly NPP and NEP of vegetation in the study area were consistent with the established variation trends (Fig. 4a). Two peaks of NEP were observed in 1 year, which appeared in May ( $30.61 \text{ g C} \cdot \text{m}^{-2} \cdot \text{a}^{-1}$ ) and August ( $27.81 \text{ g C} \cdot \text{m}^{-2} \cdot \text{a}^{-1}$ ), respectively. The NEP in these 2 months accounted for 65.74% of the total annual NEP. The lowest NEP ( $-7.34 \text{ g C} \cdot \text{m}^{-2} \cdot \text{a}^{-1}$ ) was recorded in February, accounting for 8.26% of the total annual NEP. The NEP in March–September was generally positive, indicating that the local vegetation ecosystem was a carbon sink during this period, and the carbon sequestration of the vegetation was higher than the microbial respiration of the soil. The NEP in October–February of the following year was negative, indicating that the local vegetation ecosystem was a carbon source during this period, and the carbon sequestration of the vegetation was lower than the

microbial respiration of the soil. As shown in Fig. 4a, the average NPP and NEP declined sharply in June, although the reduction of the NPP (39.73%) was significantly lower than that of the NEP (93.40%). Such variations of the monthly NPP and NEP can be explained as follows: the tableland of the Loess Plateau is a major grain supply center in Shaanxi province, and the main land use (> 70%) is crop cultivation which are mainly occupied by cereal crops, such as wheat and corn, wheat is harvested from the end of May until middle June, resulting in a drastic reduction of the vegetation coverage in June. However, the microbial respiration of the soil (HR) is increased as the temperature and soil water, from precipitation, increased in this period, thereby a sharp reduction of the NEP was observed. The inter-annual variation trend of the monthly NEP is shown in Fig. 4b, which reflects the slope of change for each month from 2003 to 2012. As revealed in Fig. 4b, the NEP of the month increases annually, except for those in April and September. The highest average growths were recorded in May, June, and July; however, only in June, the increment was significant. That is, the NEP significantly increased in June ( $P < 0.05$ ).

### Variation characteristics of the carbon sequestration efficiency of different vegetation types

The overall variation of the NPP was similar to that of the NEP for different vegetation types (Fig. 5a). The carbon sequestration capacity of different vegetation types in the region

**Table 2** The characteristics of NPP changes during 2003–2012

Statistics	NPP in different years ( $\text{g C} \cdot \text{m}^{-2} \cdot \text{a}^{-1}$ )										10 year average
	2003	2004	2005	2006	2007	2008	2009	2010	2011	2012	
Min	70.10	118.64	101.27	122.61	102.54	133.24	119.27	133.15	103.88	137.88	114.26
Max	631.94	685.23	787.23	807.68	718.01	708.89	696.21	770.23	730.88	717.58	725.39
Mean	368.23	390.29	378.30	393.72	367.58	383.98	396.00	418.21	380.44	402.93	387.97
Std	80.96	73.80	101.07	94.95	68.29	69.40	89.98	87.59	112.33	78.05	85.64
Total NPP (Tg C)	4.76	5.04	4.89	5.09	4.75	5.00	5.12	5.40	4.91	5.20	5.02

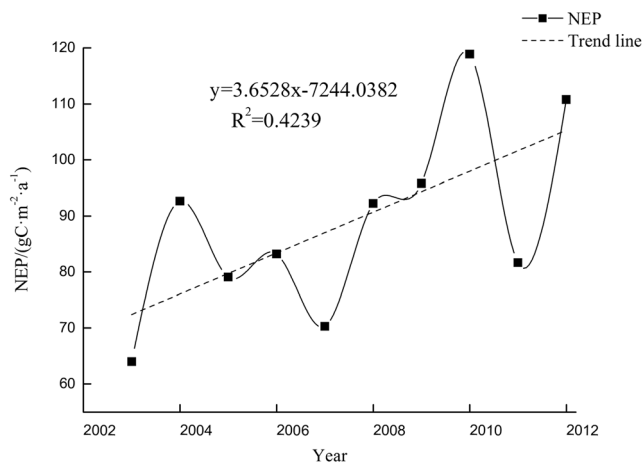


**Fig. 3** Interannual variation of vegetation NEP during 2003–2012 in the tableland of Loess Plateau

presented obvious hierarchical variations (Fig. 5a) that can be classified into three categories. The first category comprised mixed broadleaf conifer forest, evergreen broadleaf forest, and deciduous broad-leaf forest, which had annual average NEPs of 127.23, 126.29, and 112.40 g C·m<sup>-2</sup> a<sup>-1</sup>, respectively. The

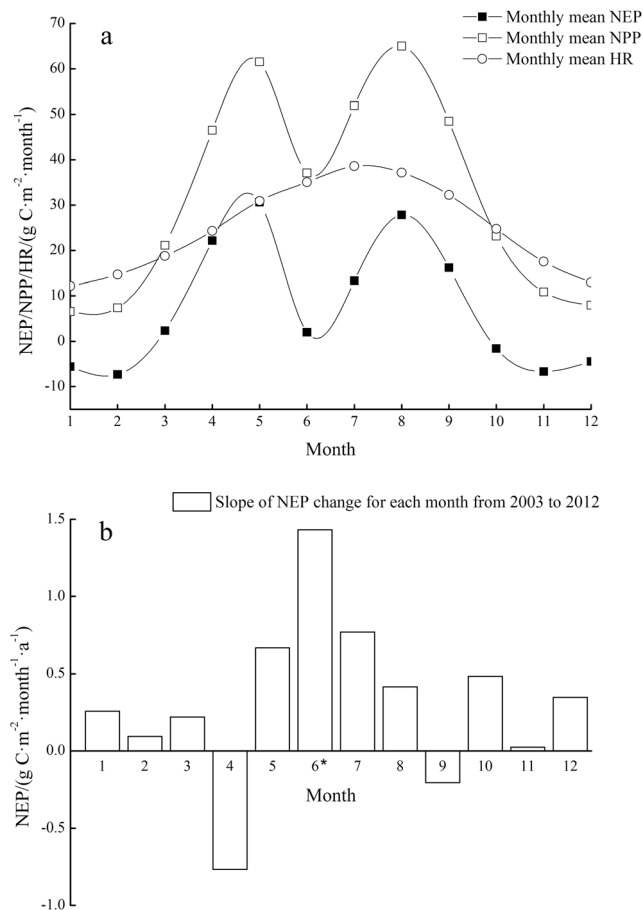


**Fig. 4** Seasonal variation of NEP, NPP, and HR (a), slope of NEP change for each month from 2003 to 2012 (b) in the tableland of Loess Plateau. \* significance at the 0.05 levels

second category consisted of cultivated land (93.40 g C·m<sup>-2</sup> a<sup>-1</sup>) and shrub forest (61.33 g C·m<sup>-2</sup> a<sup>-1</sup>). The third category included grassland (40.61 g C·m<sup>-2</sup> a<sup>-1</sup>) and bare land and sparse vegetation (14.64 g C·m<sup>-2</sup> a<sup>-1</sup>); this category demonstrated extremely poor carbon sequestration. In terms of carbon sequestration capacity, the different vegetation types can be ordered as follows: mixed broadleaf-conifer forest > evergreen broad-leaved forest > deciduous broad-leaved forest > cultivated land > shrub forest land > grassland > bare land and spare vegetation. The NEP of all vegetation types continuously improved, except for that of the shrub forest (Fig. 5b). The highest growth rate was achieved by deciduous broadleaf forest (annual growth rate of 7.89 g C·m<sup>-2</sup> a<sup>-1</sup>,  $P < 0.01$ ), followed by mixed broadleaf conifer forest (annual growth rate of 5.37 g C·m<sup>-2</sup> a<sup>-1</sup>,  $P < 0.01$ ). The NEP of shrub forest sharply declined ( $P < 0.05$ ), and the annual average reduction was 3.86 g C·m<sup>-2</sup> a<sup>-1</sup>. The NEP growth trends of the other vegetation types were insignificant because portions of cultivated land, grassland, and shrub forest were converted

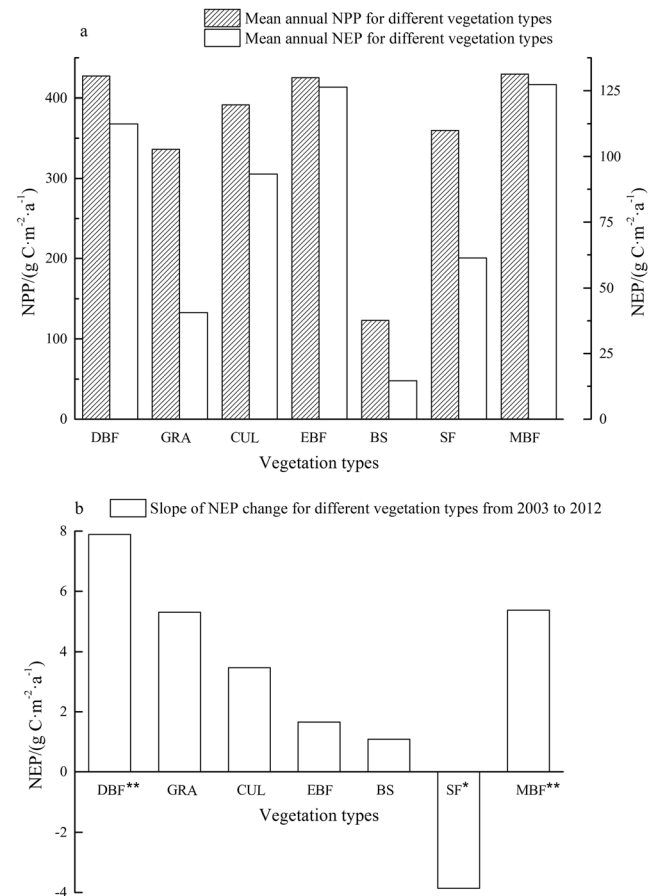


**Fig. 5** Mean annual NEP and NPP (a), variation trend of NEP (b) for different vegetation types from 2003 to 2012 in the tableland of Loess Plateau. DBF: deciduous broad-leaved forest; GRA: grassland; CUL: cultivated land; EBF: evergreen broad-leaved forest; BS: bare land and sparse vegetation; SF: shrub forest; MBF: mixed broadleaf-conifer forest. \* express significance at the 0.05 levels; \*\* express significance at the 0.01 levels

into forest at the end of twentieth century in response to afforestation and GTGP. In addition, the canopy coverage of the forest expanded as the trees aged, thereby further increasing the local vegetation coverage. In other words, the variation trend of the NEP reflected the increasing carbon sequestration capacities of the different vegetation types.

### Overall spatial distribution of vegetation carbon sequestration

The overall spatial distribution of vegetation carbon sequestration efficiency in the study area was obtained from the average NEP in 2003–2012 (Fig. 6b). A positive value indicated that the vegetation ecosystem was a carbon sink, whereas a negative value implied that the vegetation ecosystem was a carbon source. In general, the NEP presented a significantly uneven spatial distribution; high in the southwest and low in the northeast. Carbon sinks were mainly concentrated in the Baoji tableland, the southern central area of the Xianyang tableland, as well as the northwestern and northern areas of the Weinan tableland, all of which covered 86.29% of the study area. Carbon sources were distributed mainly in the middle of the Weinan tableland, the Tongchuan tableland, the Xi'an tableland, and the northern area of the Xianyang tableland, all of which covered 13.71% of the study area.

The areas with NEPs exceeding  $200 \text{ g C}\cdot\text{m}^{-2} \text{ a}^{-1}$  accounted for 7.08% of the study area and were mainly concentrated in the belt of the deciduous broad-leaved forest in the southwest side of the Baoji Tableland, and the border between the Baoji and Xianyang Tablelands (Fig. 6a, b). The areas with NEPs in the range of  $0\text{--}100 \text{ g C}\cdot\text{m}^{-2} \text{ a}^{-1}$  and  $101\text{--}200 \text{ g C}\cdot\text{m}^{-2} \text{ a}^{-1}$  occupied 41% and 38% of the study area, respectively, spreading across the entire tableland of the Loess Plateau. The areas with NEPs lower than  $0 \text{ g C}\cdot\text{m}^{-2} \text{ a}^{-1}$  accounted for 13.71% and were mainly located in the construction land of the Weinan tableland, the Tongchuan tableland, the northern region of the Xianyang tableland, and the northern central region of the Xi'an tableland.

### Inter-annual tendency of spatial variations of vegetation carbon sequestration

The variation trend of each pixel in the tableland of the Loess Plateau in 2003–2012 was calculated by unary linear regression analysis (Fig. 6c). Approximately 76% of the study area presented a steady increase in the NEP during the period. The annual NEP growth rate, which was in the range of  $1\text{--}10 \text{ g C}\cdot\text{m}^{-2} \text{ a}^{-1}$  comprised 63.24% of the total area, of which only 17.2% were statistically significant (Fig. 6d). The increased NEP areas were mainly located in the northeastern and

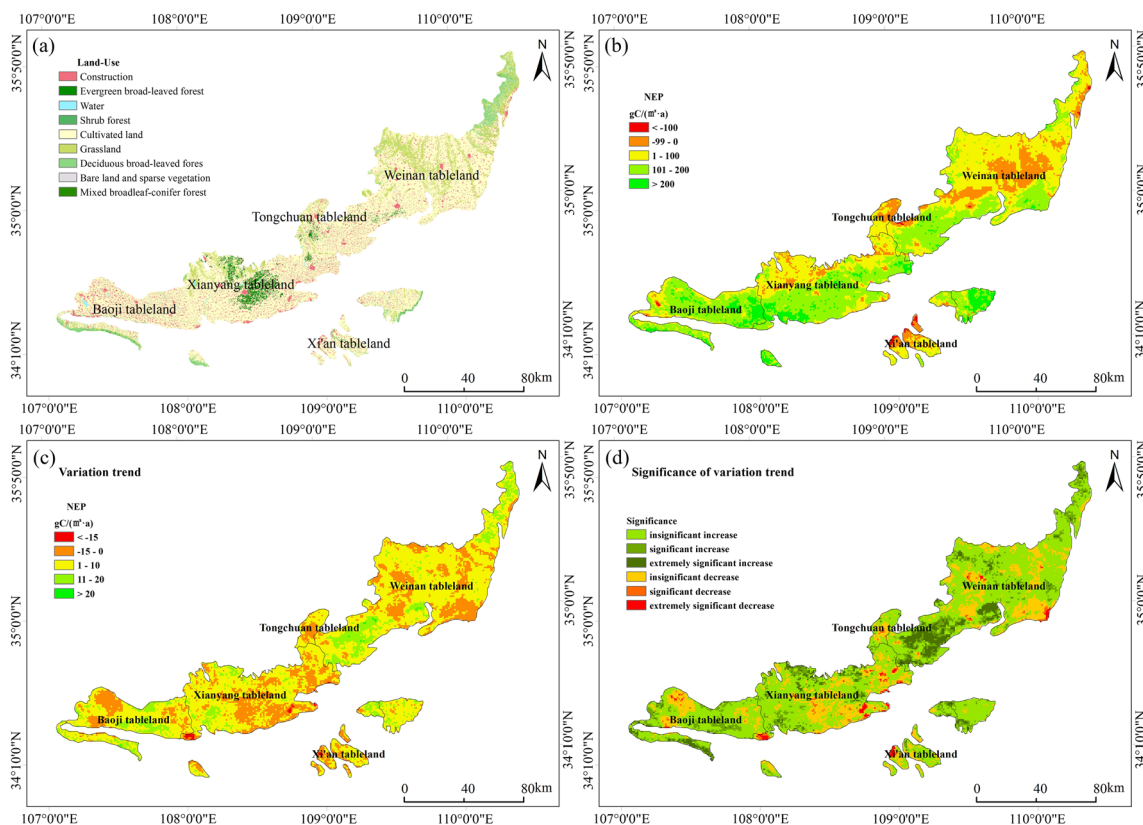


**Fig. 6** The main land-use types in the tableland of Loess Plateau (a). Spatial distribution of average NEP in the tableland of Loess Plateau (b); variation trend of annual NEP (c); and significance of variation trend (d) in the tableland of Loess Plateau during 2003–2012

southwestern regions of the Weinan tableland, the northern region of the Xianyang tableland, and the central region of the Baoji tableland, where deciduous broad-leaved forest and cultivated land were the dominant vegetation types. By contrast, areas with reduced NEPs accounted for only 24% of the total area. The NEPs of the majority of the areas were decreased by  $-15-0 \text{ g C}\cdot\text{m}^{-2} \text{ a}^{-1}$ ; only 2.4% of the areas experienced sharp reductions of the NEP. These areas were mainly located in the grassland region of the Weinan tableland, the evergreen broad-leaved forest region of the Xianyang tableland, the northern construction region of the Xi'an tableland, and the western region of the Baoji tableland, which were close to construction lands.

### Influencing factors

Figure 7 shows the extent of influence of the different variable groups on the spatial variation of the NEP, as well as their interaction and independent effects. X1, X2, X3, and X4 represented the geographic location (LON and LAT), the terrain factors (DEM, SLO, and ASP), the meteorological factors (TEM, RF, and RAD), and soil and vegetation factors (SOC and NDVI). The total explanatory ability of these variables on the NEP variation was about 91%, suggesting that some of the information(y) remained unknown and needed further investigation. Among the explained variables, soil and vegetation factors(X4) presented the strongest explanatory ability. Approximately 57% of the spatial variations of the NEP were independently caused by NDVI and SOC. Geographic location(X1) had the second strongest explanatory ability. Approximately 6% of the spatial variations were independently caused by LON and LAT. Meteorological factors (X3) had an explanatory ability of 4%, and terrain factors (X2) had the weakest explanatory ability. Only 2% of the variations were independently attributed to DEM, SLO, and ASP. Therefore, the spatial distribution of the NEP was most sensitive to soil

and vegetation factors and least sensitive to the other three types of environmental factors. This finding was reflected by small overall differences of the rest of the environmental variable groups in the study area. Therefore, the environmental variable groups can be ordered in terms of explanatory ability as follows: soil and vegetation factors > geographic location > meteorological factors > terrain factors.

Interaction effect refers to the explanatory ability of coupled environmental variables for the NEP distribution. As shown in Fig. 6, the geographic location, meteorological factors, and soil and vegetation factors cooperated well, presenting interaction effect of 13%. Geographic location, terrain factors, and soil and vegetation factors presented an interaction effect of 5%. Geographic location, terrain factors, and meteorological factors had interaction effect of 2%. Geographic location and soil and vegetation factors had an interaction effect of 2%.

Table 3 provides the significance test results and importance order of the environmental variables. The explanatory ability of NDVI was 53.56% with a strong significance at the 0.001 levels, indicating that it was the primary decisive factor of the NEP variations. The explanatory abilities of LAT, LON, and RF were 18.09%, 11.43%, and 8.33%, respectively, and were close to the 0.001 significance levels, reflecting their importance in the NEP variation. The explanatory abilities of DEM, SLO, and SOC were lower than 3% and passed the significance test at the 0.001 levels. The explanatory abilities of TEM, RAD, and ASP were lower than 1% and were below the significance levels. In particular, the explanatory ability of ASP was only 0.0064%. In order to find out the further effects of influence factors on NEP, we did a simple correlation analysis (Table 4). As we can see, only RF and NDVI made positive driven actors.

X1, X2, X3, and X4 represented the geographic location (LON and LAI), the terrain factors (DEM, SLO, and ASP), the meteorological factors (TEM, RF, and RAD), and soil and vegetation factors (SOC and NDVI), respectively.

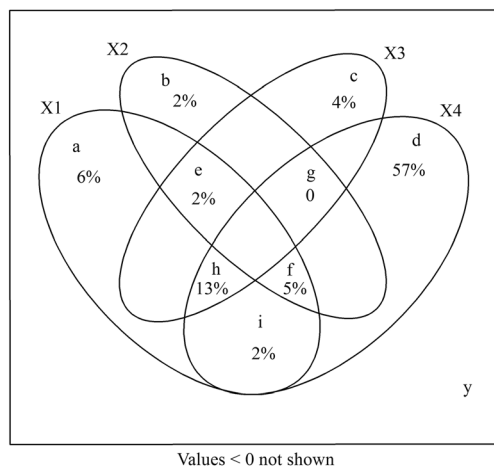


Fig. 7 Effects of different influencing variable sets on NEP in the tableland of Loess Plateau

### Discussion

#### Temporal variations of carbon sequestration efficiency

The vegetation carbon sequestration in the study area strengthened every year with an annual growth rate of 3.65 g C, despite having violent fluctuations (Table 2, Fig. 3), which agreed with the conclusion of Pan and Wen (2015). Research has showed that the negative NEP appeared in some areas of Loess Plateau for the period 1981–1998 by Cao et. al (2003), which differed from our findings. In previous studies, land cover/land use changes (e.g., deforestation and afforestation) have a significant



**Table 3** Effects of different influencing variable sets on NEP

Environmental variables	Importance order	$r^2$	Proportion	Pr(>r) <sup>z</sup>
NDVI	1	0.8357	53.56%	0.001 ***
LAI	2	0.2823	18.09%	0.001 ***
LON	3	0.1783	11.43%	0.001 ***
RAI	4	0.1300	8.33%	0.001 ***
DEM	5	0.0459	2.94%	0.002 **
SLO	6	0.0457	2.93%	0.006 **
SOC	7	0.0374	2.40%	0.006 **
TEM	8	0.0045	0.29%	0.559 <sup>ns</sup>
RAD	9	0.0004	0.03%	0.95 <sup>ns</sup>
ASP	10	0.0001	0.01%	0.991 <sup>ns</sup>

impact on changes of carbon stocks in terrestrial ecosystems (Pan et al. 2015; Tian et al. 2011; Tao et al. 2007). Furthermore, given that cultivated land is the major land use type (70%) in study area. The fluctuations in the inter-annual carbon sequestration of the cultivated land were caused by changes in the crop planting area and yield of that year, which in turn resulted from the fluctuations in the price of agricultural products. The reductions in corn and wheat yield in 2003 and 2007, respectively, were major causes of agricultural carbon sequestration reduction in those years; these findings were consistent with the study of Wang and Nan (2012) on the carbon source/sink of cultivated land in Shaanxi Province. The price of agricultural products has been steadily increasing since 2008 under market regulation and government supervision, resulting in an intensified agricultural carbon sequestration.

The NPP, NEP, and HR of vegetation in the study area changed regularly on monthly time scale (Fig. 4a). The NEP was positively correlated with NPP ( $R^2 = 0.943$ ), which indirectly indicates that the NPP play the main driving role in the carbon stocks in the northern China (Cao et al. 2003). The variations consisted of the accumulation period of the NPP ( $6.56\text{--}61.51 \text{ g C m}^{-2} \text{ a}^{-1}$ ,  $R^2 = 0.927$ ) and the NEP ( $-5.59\text{--}30.61 \text{ g C m}^{-2} \text{ a}^{-1}$ ,  $R^2 = 0.893$ ) in January–May, which was manifested by the increasing trend of the NPP and the NEP, while the consumption period in August–December, which showed a decreasing trend (Fig. 4a). The NEP increased year by year in the same month (Fig. 4b), except in April and September because of the climate warming. Under the influence of low pressure in April and September of each year, the cold and warm air will meet frequently in the tableland of Loess Plateau, resulting in continuous rainy weather. As a

result, the local maximum precipitation usually does not occur in summer but in April or September. In recent years, with global warming, this phenomenon is more prominent, the direct result is a decrease in NPP, while HR continues to increase.

### Carbon sequestration of different vegetation types and inter-annual variation

Zhang and Zhou (2008) found that the variation features of carbon sink were related to the vegetation type. Given Fig. 5, among the different vegetation types in the study area, the mixed broadleaf conifer forest presented the strongest carbon sequestration with a significant growth trend ( $P < 0.01$ ), followed by evergreen broadleaf forest and deciduous broadleaf forest ( $P < 0.01$ ). Although shrub forest exhibited a moderate carbon sequestration capacity, the growth rate drastically declined ( $P < 0.05$ ). This finding was consistent with those of Xu et al. (2009) and Hu et al. (2011). However, these conclusions cannot be directly verified without the measurement data of the NPP and the NEP for comparison in the study area. Thus, the research data were compared with measurement data for different vegetation types in the Chinese mainland (Tao et al. 2003; Zhu et al. 2007; Yuan et al. 2014). The result revealed that the NPP simulated by the CASA model was within the range of the measurement data. Several NPP values simulated by CASA were lower than the measurement data possibly because of the differences in research data, study period, model parameters, and model structure. Few measurement data are available on the NPP and NEP of vegetation in China, and these data are difficult to acquire. As such, uniform standards and methods are difficult to establish for model selection (Zhang and Zhu 2013). Future studies should discuss

**Table 4** Simple correlation between NEP and its influencing factors

	LON	LAT	DEM	SLO	ASP	TEM	RF	RAD	SOC	NDVI
NEP	-0.384**	-0.483**	-0.195**	-0.194**	-0.007	-0.061	0.328**	0.019	-0.176**	0.831**

model fitting and verification based on measurement data, and further explore the application range and differences of the simulation data.

### Spatial variations of carbon sequestration efficiency

According to the distribution of vegetation types in the tableland of Loess Plateau (Fig. 6a), carbon sources were mainly located in degenerated grassland and in urbanized and construction concentrated areas. The vegetation carbon sequestration was relatively high in the region of forest ecosystems (Fig. 6b), which contributed a large carbon storage during this time, and consistent with the results of Jianyong Ma (Ma et al. 2017). Chuluun and Ojima (2002) stated that grassland degeneration is an important carbon source process. Negative or lower NEP occurred in the Weinan tableland, Tongchuan tableland and Xianyang tableland, which comprised a large grassland area, possibly because of the emphasis on afforestation and the contempt for grassland. Economic forest accounts for excessive proportions, and grassland is being significantly reduced. In addition, the average carbon emission in Xi'an and the surrounding regions was higher than that in other regions because of the high population density. These finding also confirmed with the conclusions of Watson et al. (2000) and Dragoni et al. (2011) that land coverage changes are typically accompanied by abundant carbon exchange. Moreover, Mabicka et al. (2014) and Zhang et al. (2014) reported that increasing the vegetation coverage and changing the land use types are effective measures for protecting soil carbon pool. China has launched various national forestry ecological construction projects in the “Three-North Regions” of China since the TNSFP was implemented in 1978. The key construction areas of these projects included Tongchuan, Xianyang, most regions of Baoji and Weinan, as well as one district and one county of Xi'an. The forest coverage in Xianyang increased every year from 2003 to 2012 as a result of the construction of a farmland shelterbelt network of barren mountains and lands suitable for afforestation. Furthermore, GTGP brought about considerable changes to the ecological environment in the densely populated Tongchuan, as revealed by the reduced carbon emissions, the increased NEP of vegetation, and the reduced carbon sources. However, the comprehensive conversion of farmland into forests or grassland is challenged by the scattered distribution of GTGP project, remarkable differences in the natural geographical conditions, and imbalanced economic development. These challenges cause the slow or even negative growth of vegetation carbon sequestration efficiency. Nevertheless, carbon emissions in the study area are not fixed, given Fig. 6c, the vegetation carbon sequestration capacity of evergreen broad-leave forest and cultivated land was diminishing, and the carbon release by the main carbon sources in the grassland area was reduced over time, there

was even a significant increase ( $P < 0.05$ ) in some areas (Fig. 6d). Overall, the local vegetation coverage stabilized gradually from fluctuation, and the carbon sink capacity gradually stabilized.

### Relationship between vegetation carbon sequestration and the influencing factors

The NEP of the vegetation in the study area was jointly influenced by geographic location, the terrain, the meteorological, and soil and vegetation factors, which were consistent with the study of Kljun et al. (2007). NDVI was the most dominant influencing factor ( $R^2 = 0.8357$ ,  $P < 0.001$ ). The relationship between NEP and NDVI implied that vegetation carbon sinks were sensitive to vegetation density. That is, a higher vegetation density corresponded to a stronger carbon sequestration, the results were also suggested by Tang et al. (2013) and Mekonnen et al. (2016). The NEP was positively correlated with the RF as the second most dominant influencing factor ( $R^2 = 0.13$ ,  $P < 0.001$ ) of the NEP while the TEM was insignificant to the NEP. In view of the interactions among the influencing factors, temperature might indirectly influence the spatial variation of the NEP through vegetation growth (Hazarika et al. 2005; Nayak and Patel 2010; Mabicka et al. 2014; Liu et al. 2015; Zhou et al. 2017). The temperature in the study area was stable. Tao et al. (2006) and Ma et al. (2013) reported that the NEP in north China was mainly determined by RF and was hardly related to the temperature. China's terrestrial carbon uptake would increase with the wetter climate, not with the warming climate (Cao 2003). The study area was close to the semi-arid region in northwest China, which experienced frequent precipitation shortage. As such, water was an important limitation factor of the NEP, which was also confirmed with the conclusion of Li et al. (2017) and Tian et al. (2017). Ito (2008) stated that the annual changes in temperature and solar radiation were the main reasons for the inter-annual changes in the carbon budget in East Asia. Adequate solar radiation is available in the tableland of the Loess Plateau, making it insensitive to solar radiation. Thus, the variations of the vegetation carbon sequestration in the study area mainly resulted from geographic space differences. LAT and LON were negatively correlated with the NEP of vegetation (Table 3, Table 4). In particular, the vegetation carbon sequestration significantly declined as the LAT was increased ( $R^2 = 0.28$ ,  $P < 0.001$ ). This finding agreed with the conclusion of Zhang et al. (2015). Moreover, the decomposition rate of the SOC must be reduced to increase the carbon sinks of the terrestrial ecosystem (Xu et al. 2009), as verified by the relationship between the SOC and NEP of vegetation. The decomposition rate of the SOC directly determined the soil respiratory rate. The NEP of vegetation was affected by the excessively high decomposition rate of the SOC, thus weakening the carbon sequestration. The

terrain factors were closely related to the vegetation carbon sequestration, a result also suggested by Gong et al. (2017). The NEP of vegetation was negatively correlated with the DEM and the SLO (Table 3, Table 4). Given that the study area was mainly concentrated in plain and agricultural areas, agricultural activities had poor adaptability to places with high elevations and large slopes. No obvious relationship was detected between the SLO and the vegetation carbon sequestration. Further studies and discussions are necessary to confirm these findings. To sum, the vegetation carbon sequestration in the tableland of the Loess Plateau was the joint effect of multiple factors. Given that the NEP is the difference between the NPP and the HR, its variation is complex.

## Conclusions

Based on the CASA model and the GSMSR model, we estimated the spatial-temporal patterns of the vegetation NEP in the tableland of Loess Plateau for the period of 2003–2012. The results showed that the study area was carbon uptake and had a significantly uneven overall spatial distribution. The vegetation carbon sequestration generally increased in a fluctuational manner because of the impacts of the growth status. A series results showed that great progress had been made in local ecological restoration, the growth trend of the vegetation in the study area was improved continuously, and the terrestrial vegetation ecosystem was restored.

We further found that carbon sequestration capacity of terrestrial ecosystems was related to vegetation cover types, especially the high carbon uptake capacity of forest ecosystems, but low in construction area. The high carbon sequestration capacity of forest ecosystems and carbon footprint expansion caused by grassland degradation indicates that measures such as afforestation and returning farmland to forests (grassland) have important ecological significance for local carbon balance. Furthermore, the carbon sequestration capacity of vegetation is also promoted or inhibited by single or multiple factors, such as geographic position, terrain, meteorology, and soil and NDVI.

**Funding information** This work was supported by the National Program on Key Research Project (2016YFC0501703), Basic Research program of Natural Science in Shaanxi (2017JZ008), and Open Foundation of Key Laboratory for Agricultural Environment, Ministry of Agriculture, P.R. China.

## References

Bond-Lamberty B, Wang C, Gower ST (2010) A global relationship between the heterotrophic and autotrophic components of soil respiration? *Global Change Biology* 10(10): 1756–1766

- Cao MK, Prince SD, Li KR, Tao B, Small J, Shao XM (2003) Response of terrestrial carbon uptake to climate interannual variability in China. *Global Change Biology* 9(4): 536–546
- Carvalho N, Reichstein M, Collatz GJ, Mahecha MD, Migliavacca M, Neigh CSR, Tomelleri E, Benali AA, Papale D, Seixas J (2010) Deciphering the components of regional net ecosystem fluxes following a bottom-up approach for the Iberian Peninsula. *Biogeosciences* 7(11):3707–3729
- Chuluun T, Ojima D (2002) Land use change and carbon cycle in arid and semi-arid lands of east and Central Asia. *Sci China C Life Sci* 45(1):48–54
- Dragoni D, Schmid HP, Wayson CA, Potter H, Grimmer C, Susan B, Randolph JC (2011) Evidence of increased net ecosystem productivity associated with a longer vegetated season in a deciduous forest in south-Central Indiana. *USA Glob Change Biol* 17(2):886–897
- Fang JY, Chen AP, Peng CH (2001) Changes in forest biomass carbon storage in China between 1949 and 1998. *Science* 292(5525):2320–2322
- Fang JY, Guo ZD, Piao SL, Chen AP (2007) Estimation of carbon sink of terrestrial vegetation in China during 1981–2000. *Sci China (Ser D)* 37(6):804–812
- Field CB, Randerson JT, Malmström CM (1995) Global net primary production: combining ecology and remote sensing ☆. *Remote Sens Environ* 51(1):74–88
- Gong J, Zhang Y, Qian CY (2017) Temporal and spatial distribution of net ecosystem productivity in the Bailongjiang watershed of Gansu Province. *Acta Ecol Sin* 37(15):5121–5128
- Hazarika MK, Yasuoka Y, Ito A, Dye D (2005) Estimation of net primary productivity by integrating remote sensing data with an ecosystem model. *Remote Sens Environ* 94(3):298–310
- Hu B, Sun R, Chen YJ, Feng LC, Sun L (2011) Estimation of the net ecosystem productivity in Huang-Huai Hai region combining with biome-BGC model and remote sensing data. *J Nat Resources* 26(12):2061–2071
- Ito A (2008) The regional carbon budget of East Asia simulated with a terrestrial ecosystem model and validated using Asia flux data. *Agric Forest Meteorol* 148(5):738–747
- Kljun N, Black TA, Griffis TJ, Barr AG, Gaumont-Guay D, Morgenstern K, Mccaughy JH, Nesic Z (2007) Response of net ecosystem productivity of three boreal Forest stands to drought. *Ecosystems* 10(6): 1039–1055
- Li GY, Han HY, Du Y, Hui DF, Xia JY, Niu SL, Li XN, Wan SQ (2017) Effects of warming and increased precipitation on net ecosystem productivity: a long-term manipulative experiment in a semiarid grassland. *Agric Forest Meteorol* 232:359–366
- Liu CY, Dong XF, Liu YY (2015) Changes of NPP and their relationship to climate factors based on the transformation of different scales in Gansu, China. *Catena* 125:190–199
- Liu GH, Fu BJ, Fang JY (2010) Carbon dynamics of Chinese forests and its contribution to global carbon balance. *Acta Ecol Sin* 20(5): 733–740
- Luo L, Wang ZM, Mao DH, Lou YJ, Ren CY, Song KS (2012) Temporal and spatial pattern of grassland net primary productivity in Western Songnen plain. *Chin J Grassland* 34(1):5–11
- Ma MG, Wang J, Wang XM (2006) Advance in the inter-annual variability of vegetation and its relation to climate based on remote sensing. *J Remote Sens* 10(3):421–431
- Ma JY, Gu XP, Huang M, Yu F (2013) Temporal-spatial distribution of net ecosystem productivity in Guizhou during the recent 50 years. *Ecol Environ Sci* 22(9):1462–1470
- Ma JY, Herman HS, Yan XD, Cao CG, Wu S, Fang J (2017) Evaluating carbon fluxes of global forest ecosystems by using an individual tree-based model FORCCHN. *Sci Total Environ* 586:939–951
- Mabicka OR, Copard Y, Sebag D, Abdourhamane TA, Boussafir M, Bichet V, Garba Z, Guillon R, Petit C, Rajot JL, Durand A (2014) Carbon sinks in small Sahelian lakes as an unexpected effect of land

- use changes since the 1960s (Saga Gorou and Dallol Bosso, SW Niger). *Catena* 114:1–10
- Mekonnen ZA, Grant RF, Schwalm C (2016) Contrasting changes in gross primary productivity of different regions of North America as affected by warming in recent decades. *Agric Forest Meteorol* 5:218–219(1–2):50–64
- Mu SJ, Zhou KX, Chen YZ, Yang Q, Li JL (2014) Net ecosystem productivity dynamics of grassland communities on the typical steppe of Inner Mongolia. *Chin J Ecol* 33(4):885–895
- Nayak RK, Patel NV (2010) Estimation and analysis of terrestrial net primary productivity over India by remote-sensing-driven terrestrial biosphere model. *Environ Monit Assess* 170:195–213
- Oksanen JF, Blanchet R, Kindt P, Legendre, and et al (2010) *vegan*: community ecology package. R package **version 1.17-3**. <http://vegan.r-forge.r-project.org/>
- Pan JH, Wen Y (2015) Estimation and spatial-temporal characteristics of carbon sink in the arid region of Northwest China. *Acta Ecol Sin* 35(23):7718–7728
- Pan Y, Li X, Gong P, He C, Shi P, Pu R (2003) An integrative classification of vegetation in China based on NOAA AVHRR and vegetation-climate indices of the Holdridge life zone. *Int J Remote Sens* 24(5):1009–1027
- Pan SF, Tian HQ, Lu CQ, Dangal SRS, Liu ML (2015) Net primary production of major plant functional types in China: vegetation classification and ecosystem simulation. *Acta Ecol Sin* 35(2):28–36
- Pang R, Gu FX, Zhang YD, Hou ZH, Liu SR (2012) Temporal-spatial variations of net ecosystem productivity in alpine area of southwestern China. *Acta Ecol Sin* 32(24):7844–7856
- Piao SL, Fang JY, He JS, Xiao Y (2004) Spatial distribution of grassland biomass in China. *Acta Phytocologica Sin* 28(4):491–498
- Potter CS, Randerson JT, Field CB, Matson PA, Vitousek PM, Mooney HA, Klooster SA (1993) Terrestrial ecosystem production: A process model based on global satellite and surface data. *Global Biogeochemical Cycles* 7(4): 811–841
- Raich JW, Potter CS (1995) Global patterns of carbon dioxide emissions from soils. *Glob Biogeochem Cycles* 9:23–36
- Raich JW, Potter CS, Bhagawati D (2002) Interannual variability in global soil respiration, 1980–94. *Glob Chang Biol* 8:800–812
- Ran YH, Li X, Lu L (2009) China land cover Classification at 1 km spatial resolution based on a multi-source data fusion approach. *Adv Earth Science* 24(2):192–203
- Ran YH, Li X, Lu L, Li ZY (2012) Large-scale land cover mapping with the integration of multi-source information based on the Dempster–Shafer theory. *Int J Geogr Inf Sci* 26(1):169–191
- Ren XL, He HL, Zhang L (2017) Net ecosystem production of alpine grasslands in the Three-River Headwaters Region during 2001–2010. *Res Environ Sci*, 2017 30(1):51–58
- Russell G, Jarvis PG, Monteith JL, Russell G, Marshall B, Jarvis PG (1989) Absorption of radiation by canopies and stand growth. *Plant Canopies Their Growth & Function* 57:21–39
- Shi ZH (2015) Spatial-temporal simulation of vegetation carbon sink and its influential factors based on CASA and GSMSR model in Shaanxi Province. Northwest of a & F University. Tang, J, Jiang, Y, Li, Z, Y. Zhang, N, Hu, M. 2013. Estimation of vegetation net primary productivity and carbon sink in western Jilin province based on CASA model. *J Arid Land Resour Environ* 27(4):1–7
- Sun R, Zhu QJ (2001) Estimation of net primary productivity in China using remote sensing data. *J Geogr Sci* 11(1):14–23
- Tang J, Jiang Y, Li ZY, Zhang N, Hu M (2013) Estimation of vegetation net primary productivity and carbon sink in western Jilin province based on CASA model. *Journal of Arid Land Resources and Environment* 27(4):1–7
- Tao B, Li KR, Shao XM, Cao MK (2003) Temporal and spatial pattern of net primary production of terrestrial ecosystems in China. *Acta Geograph Sin* 58(3):372–380
- Tao B, Cao MK, Li KR, Gu FX, Ji JJ, Huang M, Zhang LM (2006) Spatial patterns and changes of terrestrial net ecosystem productivity during 1981–2000 in China. *Sci China Ser D Earth Sci* 36(12): 1131–1139
- Tao B, Cao MK, Li KR, Gu FX, Ji JJ, Huang M, Zhang LM (2007) Spatial patterns of terrestrial net ecosystem productivity in China during 1981–2000. *Sci China Ser D Earth Sci* 50(5):745–753
- Tian HQ, Melillo J, Lu CQ, Kicklighter D, Liu ML, Ren W, Xu XF, Chen GS, Zhang C, Pan SF (2011) China's terrestrial carbon balance: contributions from multiple global change factors. *Glob Biogeochem Cycles* 25(1):GB1007–GB1022
- Tian HQ, Xu XF, Song X (2017) Drought impacts on terrestrial ecosystem productivity. *J Plant Ecol* 31(2):231–241
- Wang GB, Nan L (2012) Research on the Spatio-temporal difference of carbon source/sink of arable land resource use in Shaanxi Province. *Chin Agric Sci Bull* 28(02):245–249
- Watson RT, Noble IR, Bolin B, Ravindranath NH, Verardo DJ, Dokken DJ, Watson RT, Noble IR, Bolin B, Ravindranath NH (2000) *Land use, land-use change and forestry: a special report of the intergovernmental panel on climate change*, 333 pp. [26]
- Woodwell GM, Whittaker RH, Reiners WA, Likens GE, Delwiche CC, Botkin DB (1978) The biota and the world carbon budget. *Science* 199(4325):141–146
- Xu DF, Wang RH, Li YX, Zhang H (2009) Review on carbon cycle in terrestrial ecosystem and its influenced factors. *Chin J Agrometeorol* 30(4):519–524
- Yu GR, Zheng ZM, Wang QF, Fu YL, Jie Z, Sun XM, Wang YS (2010) Spatiotemporal pattern of soil respiration of terrestrial ecosystems in China: the development of a geostatistical model and its simulation. *Environ Sci Technol* 44(16):6074–6080
- Yuan QZ, Wu SH, Zhao DS, Dai EF, Chen L, Zhang L (2014) Modeling net primary productivity of the terrestrial ecosystem in China from 1961 to 2005. *J Geogr Sci* 24(1):3–17
- Zhan XY, Yu GR, Zheng ZM, Wang QF (2012) Carbon emission and spatial pattern of soil respiration of terrestrial ecosystems in China: based on Geostatistic estimation of flux measurement. *Prog Geogr* 31(1):97–108
- Zhang F, Zhou GS (2008) Spatial-temporal variations in net primary productivity along Northeast China transect (NECT) from 1982 to 1999. *J Plant Ecol (Chinese Version)* 32(4):798–809
- Zhang YF, Zhu N (2013) Study on the balance between carbon source/sink and ecological surplus using CASA model in Yulin. *Sci Agric Sin* 46(24):5163–5172
- Zhang XQ, Wu SH, He Y, Hou ZH (2005) Forests and forestry activities in relations to emission mitigation and sink enhancement. *Sci Silvae Sin* 41(6):150–156
- Zhang YD, Pang R, Gu FX, Liu SR (2013) Temporal-spatial variation of heterotrophic respiration in alpine area of southwestern China. *Acta Ecol Sin* 33(16):5047–5057
- Zhang WT, Huang B, Luo D (2014) Effects of land use and transportation on carbon sources and carbon sinks: a case study in Shenzhen, China. *Landsc Urban Plan* 122:175–185
- Zhang QG, Zhang YJ, Xiong H (2015) Influence factors of Forest ecosystem carbon sequestration and its regulation measurements in Jiangxi Province. *Jiangxi Science* 33(5):696–702
- Zhao JF, Yan XD, Jia GS (2009) Changes in carbon budget of Northeast China forest ecosystems under future climatic scenario. *Chin J Ecol* 28(5):781–787
- Zheng ZM, Yu GY, Sun XM, Li SG, Wang YS, Wang YH, Fu YL, Wang QF (2010) Spatio-temporal variability of soil respiration of Forest ecosystems in China: Influencing factors and evaluation model. *Environ Manag* 46:633–642
- Zhou W, Mu FY, Gang CC, Guan DJ, He JF, Li JL (2017) Spatio-temporal dynamics of grassland net primary productivity and their relationship with climatic factors from 1982 to 2010 in China. *Acta Ecol Sin* 37(13):4335–4345

- Zhu WQ, Pan YZ, He H, Yu DY, Hu HB (2006) Simulation of maximum light utilization ratio of typical vegetation in China. *Chin Sci Bull* 51(6):700–706
- Zhu WQ, Pan YZ, Zhang JS (2007) Estimation of net primary productivity of Chinese terrestrial vegetation based on remote

sensing. *J Plant Ecol* (formerly *Acta Phytocologica Sinica*) 31(3):413–424

**Publisher's note** Springer Nature remains neutral with regard to jurisdictional claims in published maps and institutional affiliations.